Electronic Supplementary Material (ESI) for ChemComm.

Supporting Information for

Enhance and Control of the Selectivity in Light-driven Ketone versus Water Reduction using Aminopyridine Cobalt Complexes

Arnau Call,[a] and Julio Lloret-Fillol[a,b]*

[a] Institute of Chemical Research of Catalonia (ICIQ), The Barcelona Institute of Science and Technology, Avinguda Països Catalans 16, 43007 Tarragona, Spain. jlloret@iciq.es

[b] Catalan Institution for Research and Advanced Studies (ICREA), Passeig Lluïs Companys, 23, 08010, Barcelona (Spain).

EXPERIMENTAL SECTION

1. Material and reagents

Reagents and solvents were purchased from commercial sources as used as received unless otherwise stated. Triethylamine (Et_3N) $\geq$ 99 % purity was purchased from Sigma-Aldrich® and distilled and degassed before used. Photosensitizers $[Ir(bpy)(ppy)_2]PF_6$ (**PS_{Ir}**),[1] and $[Cu(bathocuproine)(Xantphos)]PF_6$ (**PS_{Cu}**)[2] were synthesized according to literature procedures. Anhydrous acetonitrile was purchased from Scharlab. Water (18.2 MΩ·cm) was purified with a Milli-Q Millipore Gradient AIS system. All solvents were strictly degassed and stored under anaerobic conditions.

2. Instrumentation

Nuclear magnetic resonance (NMR) spectra were recorded on Bruker Fourier300, AV400, AV500 and AVIII500 spectrometers using standard conditions (300 K). All ^1H chemical shifts are reported in ppm and have been internally calibrated to the residual protons of the deuterated solvent. The ^{13}C chemical shifts have been internally calibrated to the carbon atoms of the deuterated solvent. The coupling constants were measured in Hz.

Elemental analyses were performed using a CHNS-O EA-1108 elemental analyzer from Fisons.

UV/Vis spectra were recorded on an Agilent 8453 diode array spectrophotometer (190-1100 nm range) in 1 cm quartz cells. A cryostat from Unisoku Scientific Instruments was used for the temperature control.

Mass Spectrometry. Electrospray ionization mass spectrometry (ESI-MS) experiments were performed on a Bruker Daltonics Esquire 3000 Spectrometer using a 1 mM solution of the analyzed compound, by introducing the sample directly into the ESI-source using a syringe. High resolution mass spectra (HRMS) were recorded on a Bruker MicroTOF-Q IITM instrument with an ESI source. Samples were introduced into the mass spectrometer ion source by direct infusion through a syringe pump and were externally calibrated using sodium formate.

Gas chromatography analysis. The analysis and quantification of the starting materials and products were carried out on an Agilent 7820A gas chromatograph (HP5 column, 30 m or Cyclosil-B column, 30 m) and a flame ionization detector.

Parallel Pressure Transducer Hardware. The parallel pressure transducer that we used for these studies is the same that previously was developed and described for water oxidation studies.[3] This is composed by 8 differential pressure transducers (Honeywell-ASCX15DN, ± 15 psi) connected to a hardware data-acquisition system (base on Atmega microcontroller) controlled by a home-developed software program. The differential pressure transducer Honeywell-ASCX15DN is a 100 microseconds response, signal-conditioned (high level span, 4.5 V) output, calibrated and temperature compensated (0 ºC to 70 ºC) sensor. The differential sensor has two sensing ports that can be used for differential pressure

measurements. The pressure calibrated devices to within ± 0.5 matm was offset and span calibrated *via* software with a high precision pressure transducer (PX409-030GUSB, 0.08 % Accuracy). Each of the 8 differential pressure transducers (Honeywell-ASCX15DN, ±15 psi) produce a voltage outputs that can directly transformed to a pressure difference between the two measuring ports. The voltage outputs were digitalized with a resolution of 0.25 matm from 0 to 175 matm and 1 matm from 176 to 1000 matm using an Atmega microcontroller with an independent voltage auto-calibration. Firmware Atmega microcontroller and control software were home-developed. The sensitivity of H_2 analytics allows quantifying the gas formed when low H_2 volumes are generated. Therefore, it could not be discarded that small amounts of H_2 were produced by inactive complexes.

Gas chromatography identification and quantification of gases. Gases at the headspace were analyzed with an Agilent 7820A GC System equipped with columns Washed Molecular Sieve 5A, 2m x 1/8'' OD, Mesh 60/80 SS and Porapak Q, 4m x 1/8'' OD, SS. Mesh: 80/100 SS and a Thermal Conductivity Detector. The quantification of the H_2 obtained was measured through the interpolation of a previous calibration using different H_2/N_2 mixtures.

Light source. The reactions were performed using Royal-Blue (λ = 447±20 nm) LUXEON Rebel ES LED, Mounted on a 10 mm Square Saber - 1030 mW @ 700 mA (Datasheet: https://www.luxeonstar.com/assets/downloads/ds68.pdf) as a light source.

3. Experimental procedures

3.1. General procedure employed in reaction screening conditions for the light-driven reduction of compounds. All catalytic reactions were conducted in a vigorous stirring under irradiation for 5 hours in 15 mL capped vials with a septum under nitrogen atmosphere at 30 ºC, unless otherwise indicated. Catalytic assays using $\mathbf{PS_{Ir}}$ as chromophore were performed in MeCN:H_2O:Et_3N (2:8:0.2 mL) reaction mixture, substrate (16.5 mM), $\mathbf{PS_{Ir}}$ (2.5 μmol, 2 mol%), $\mathbf{1^H}$ (3.8 μmol, 3 mol%). Catalytic reactions carried out using $\mathbf{PS_{cu}}$ as chromophore were performed in MeCN:H_2O:Et_3N (4:6:0.2 mL) reaction mixture, **3a** (2.0-49.5 mM), $\mathbf{PS_{Cu}}$ (2.5 μmol), $\mathbf{1^H}$ (1.7 μmol). A 447 nm LED was employed as a light source. 1,3,5-trimethoxybenzene was added as internal standard after the reaction and the reaction was quenched by adding 2 mL of CH_2Cl_2. The crude reaction mixtures were purify by extraction with CH_2Cl_2 (3 x 3 mL), the combined organic layers were dried over $MgSO_4$ and passed through a silica plug which was eluded with AcOEt. The resulting organic solution was subjected to GC analysis to determine the conversion of **3a** and the yield of the desired products **3b**.

3.2. Gas-evolution monitoring studies. Each experiment was conducted in a 20 mL volume-calibrated-vial caped with a septa equipped with stir-bars and containing the solvent mixture and reagents. Each reaction vial was connected to one of the ports of a differential

pressure transducer sensor (Honeywell-ASCX15DN) and the other port to a reference reaction. Reference reactions, have all components of the reaction except the catalyst. The reaction and reference vials are kept under the same experimental conditions to compensate the noise due to temperature-pressure fluctuations. In order to ensure a constant and stable irradiation, the LED sources were equipped with a water refrigeration system. This is composed for a refrigerated aluminium block by a Huber cryothermostat (refrigeration system, Minichiller -40ºC-20ºC). This block is shaken by an Orbital Shaker (IKA KS 260 Basic Package) which provides the agitation of the reaction vessels during the irradiation time. The aluminium block accommodates 16 vials (20 mL) capped with septum in which the reaction takes place. Each vial is submitted and located over a LED irradiation source (Royal-Blue Rebel LEDs (λ = 447±20 nm). The reaction began when the LEDs were turned on. At this point, the hydrogen evolved from the reactions was monitored by recording the increase in pressure of the headspace (1 second interval). The pressure increment is the result of the difference in pressure between the reaction and reference vials. After the hydrogen evolution reached a plateau the amount of the gas formed was measured equilibrating the pressure between reaction and reference vials. The gasses at the headspace of reaction vials and references in each of the reactions were quantified by the analysis of an aliquot of gas at the headspace (0.2 mL) by gas chromatography.

4. Synthesis of the ligands and complexes

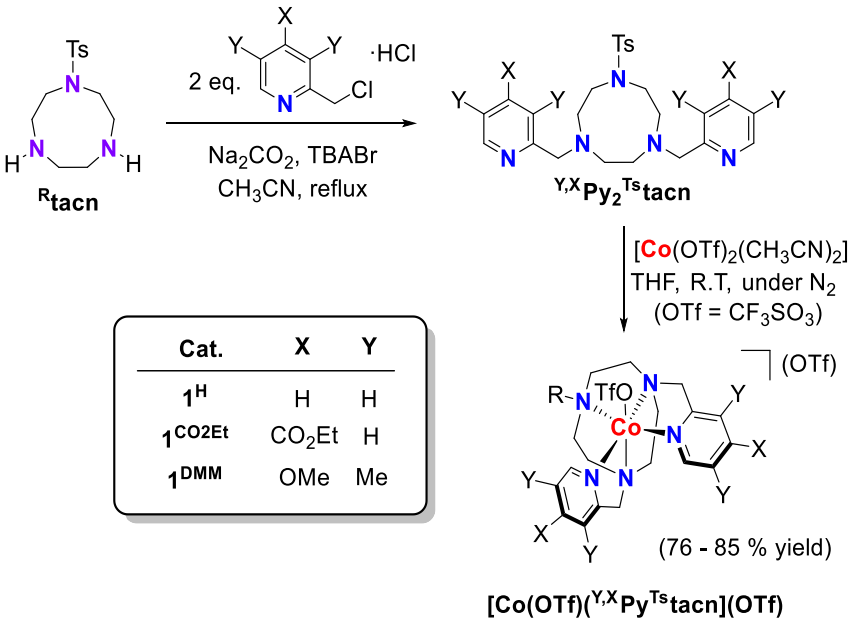

Cat.	X	Y
1^{H}	H	H
1^{CO2Et}	CO_2Et	H
1^{DMM}	OMe	Me

Scheme SI. 1. General scheme for the straightforward preparation of ligands and complexes herein studied.

4.1. Synthesis of 4,7-bis(4-methoxy-3,5-dimethyl-pyridine-2-ylmethyl)-7-(p-toluenesulfonyl)- 1,4,7-triazacyclononane, ($^{Me,OMe}Py_2{}^{Ts}tacn$)

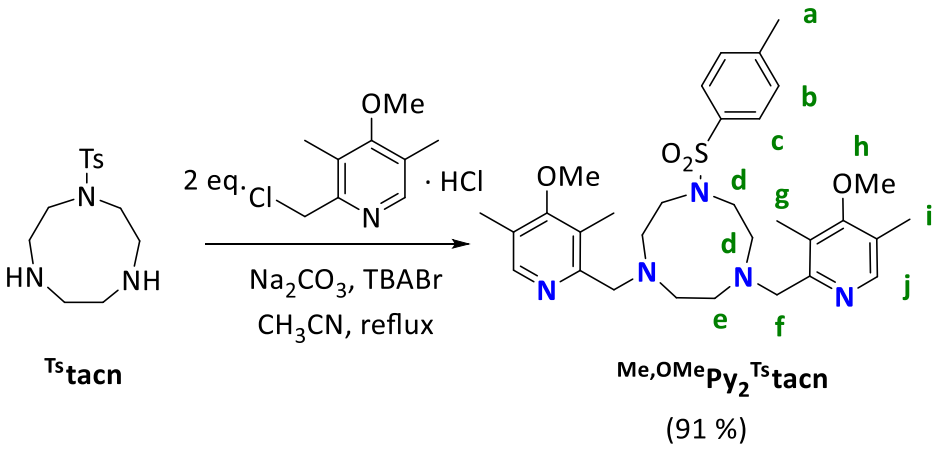

^{Ts}**tacn** ^{Me,OMe}**Py$_2$**^{Ts}**tacn**

(91 %)

Scheme SI. 2. Synthesis of $^{Me,OMe}Py_2{}^{Ts}tacn$.

2-Chloromethyl-4-methoxy-3,5-dimethylpyridine hydrochloride (0.94 g, 4.24 mmol), ^{Ts}tacn (0.60 g, 2.12 mmol) and anhydrous acetonitrile (40 mL) were mixed in a 100 mL flask. Na_2CO_3 (1.20 g) and tetrabutylammonium bromide (TBABr, 80 mg) were added directly as solids and the resulting mixture was heated at reflux for 22 hours under N_2. After cooling at room temperature, the resulting orange mixture was filtered and the filter cake was washed with CH_2Cl_2. The combined filtrates were evaporated under reduce pressure. To the resulting residue, 2 M NaOH (15 mL) was added and the mixture was extracted with CH_2Cl_2 (4 x 40 mL). The combined organic layers were dried over $MgSO_4$ and the solvent was removed under reduced pressure. The resulting residue was treated with *n*-hexane (100 mL) and stirred for 12 hours. The mixture was filtered and the solvent from the yellow filtrates was removed under reduced pressure to yield 1.12 g of a pale yellow solid (1.93 mmol, 91 %). ^{1}H-NMR ($CDCl_3$, 300 MHz, 300 K) δ, ppm: 8.11 (s, 2H, **H$_j$**), 7.56 (d, 2H, ^3J(H,H)= 8.2 Hz, **H$_c$**), 7.23 (d, 2H, ^3J(H,H)= 8.2 Hz, **H$_b$**), 3.72 (s, 10H, **H$_f$** + **H$_h$**), 3.00-3.03 (m, 8H, **H$_d$**), 2.64 (s, 4H, **H$_e$**), 2.40 (s, 3H, **H$_a$**), 2.30 (s, 6H, **H$_g$**), 2.22 (s, 6H, **H$_i$**). ^{13}C-NMR ($CDCl_3$, 300 MHz, 300 K) δ, ppm: 164.10, 157.27, 148.34, 142.82, 135.80, 129.46, 127.08, 126.10, 125.06, 62.95, 59.78, 56.18, 56.01, 50.23, 21.44, 13.22, 11.15. ESI-MS: *m/z*: 582.4 $[M+H]^+$, 291.7 $[M+2H]^{2+}$. Anal. Calcd for $C_{31}H_{43}N_5O_4S$: C, 64.00; N, 12.04; H, 7.45 %. Found: C, 64.36; N, 11.82; H, 7.62 %.

4.2. Synthesis of 4,7-bis(4-ethoxycarbonyl-2-pyridylmethyl)-7-(p-toluenesulfonyl)-1,4,7-triazacyclononane, ($^{H,CO2Et}Py_2^{Ts}tacn$)

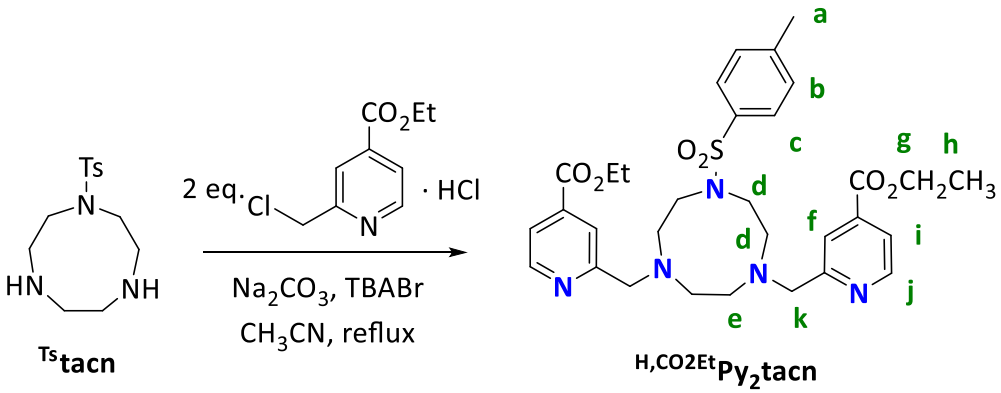

Scheme SI. 3. Synthesis of $^{H,CO2Et}Py_2^{Ts}tacn$.

Ligand $^{H,CO2Et}Py_2^{Ts}tacn$ was synthesized following the same synthetic procedure that in $^{Me,OMe}Py_2^{Ts}tacn$ (93 %). ^{1}H-NMR ($CDCl_3$, 300 MHz, 300 K) δ, ppm: 8.66 (dd, ^3J(H,H)= 5.1 Hz, $^3J'$(H,H)= 0.8 Hz, 2H, **H$_j$**), 8.00 (dd, ^3J(H,H)= 1.5 Hz, $^3J'$(H,H)= 0.8 Hz, 2H, **H$_f$**), 7.70 (dd, ^3J(H,H)= 5.1 Hz, $^3J'$(H,H)= 1.6 Hz, 2H, **H$_i$**), 7.65 (d, ^3J(H,H)= 8.3 Hz, 2H, **H$_c$**), 7.27 (d, ^3J(H,H)= 8.3 Hz, 2H, **H$_b$**), 4.40 (q, ^3J(H,H)= 7.1 Hz, 4H, **H$_c$**), 3.95 (s, 4H, **H$_k$**), 3.27-3.17 (m, 8H, **H$_d$**), 2.84 (s, 4H, **H$_e$**), 2.40 (s, 3H, **H$_a$**), 1.39 ((t, ^3J(H,H)= 7.1 Hz, 6H, **H$_h$**). ^{13}C-NMR ($CDCl_3$, 300 MHz, 300K) δ, ppm: 165.64, 161.54, 150.11, 143.31, 138.45, 136.27, 129.91, 127.39, 122.71, 121.42, 63.67, 62.04, 56.00, 55.81, 51.03, 21.75, 14.49. ESI-MS: *m/z*: 610.3 $[M+H]^+$. Anal. Calcd for $C_{31}H_{39}N_5O_6S$: C, 61.07; N, 11.49; H, 6.45 %. Found: C, 60.95; N, 11.39; H, 6.36 %.

4.3. Synthesis of [Co(OTf)($^{H,CO2Et}Py_2^{Ts}tacn$)](OTf) (1^{CO2Et})

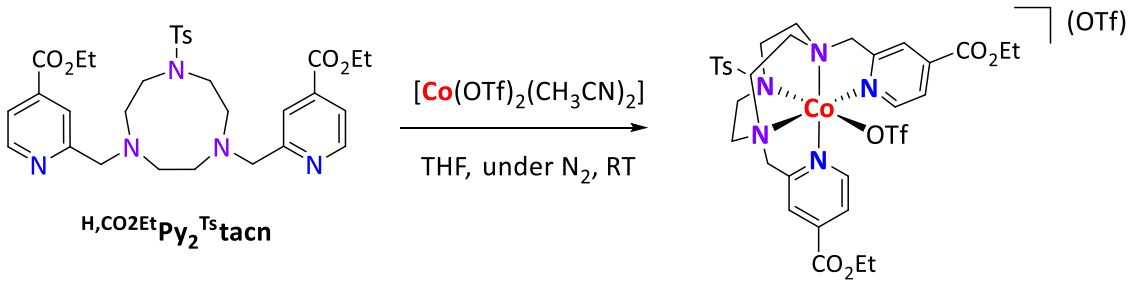

Scheme SI. 4. Synthesis of **1^{CO2Et}**.

In a glovebox, a solution of $[Co(OTf)_2(MeCN)_2]$ (216 mg, 0.492 mmol) in anhydrous THF (1 mL) was added dropwise to a vigorously stirred solution of $^{H,CO2Et}Py_2^{Ts}tacn$ (300 mg, 0.492 mmol) in THF (1 mL). After few minutes, the solution become cloudy and a brown precipitate appeared. After stirring for an additional 2 hours the solution was filtered off and the resulting solid dried under vacuum. The obtained solid was dissolved in CH_2Cl_2 (3 mL), filtered through

Celite© and crystallized by slow diffusion of diethyl ether into CH_2Cl_2 yielding a 362 mg of a brown crystalline solid (0.373 mmol, 76 %). Anal. Calcd for $C_{33}H_{39}CoF_6N_5O_{12}S_3$: C, 41.00; N, 7.24; H, 4.07 %. Found: C, 40.89; N, 7.20; H, 4.14 %. HR-ESI-MS (m/z): 817.1469 $[M - OTf]^+$, 334.0976 $[M\text{-}2\cdot OTf]^{2+}$.

4.4. *Synthesis of* [Co(OTf)(*Me,OMe*Py$_2$*Ts*tacn)](OTf) *(1^{DMM})*

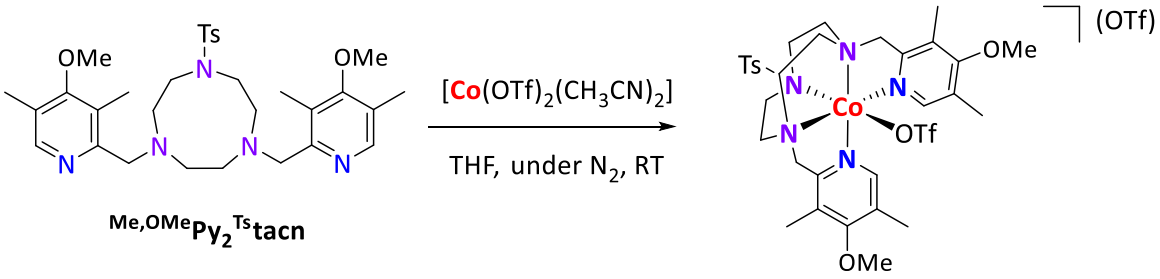

Me,OMePy$_2$Ts tacn

[Co(OTf)(Me,OMePy$_2$Ts tacn)](OTf) (1^{DMM})

(85 %)

Scheme SI. 5. Synthesis of **1^{DMM}**.

1^{DMM} as a crystalline pink solid was synthesized following the same synthetic procedure as described for complex **1^{CO2Et}** (85 %). Anal. Calcd for $C_{33}H_{43}CoF_6N_5O_{10}S_3$: C, 42.22; N, 7.46; H, 4.62 %. Found: C, 42.53; N, 7.64; H, 4.59 %. HR-ESI-MS (m/z): 789.1889 $[M - OTf]^+$, 320.1190 $[M\text{-}2\cdot OTf]^{2+}$.

5. Characterization of the complexes

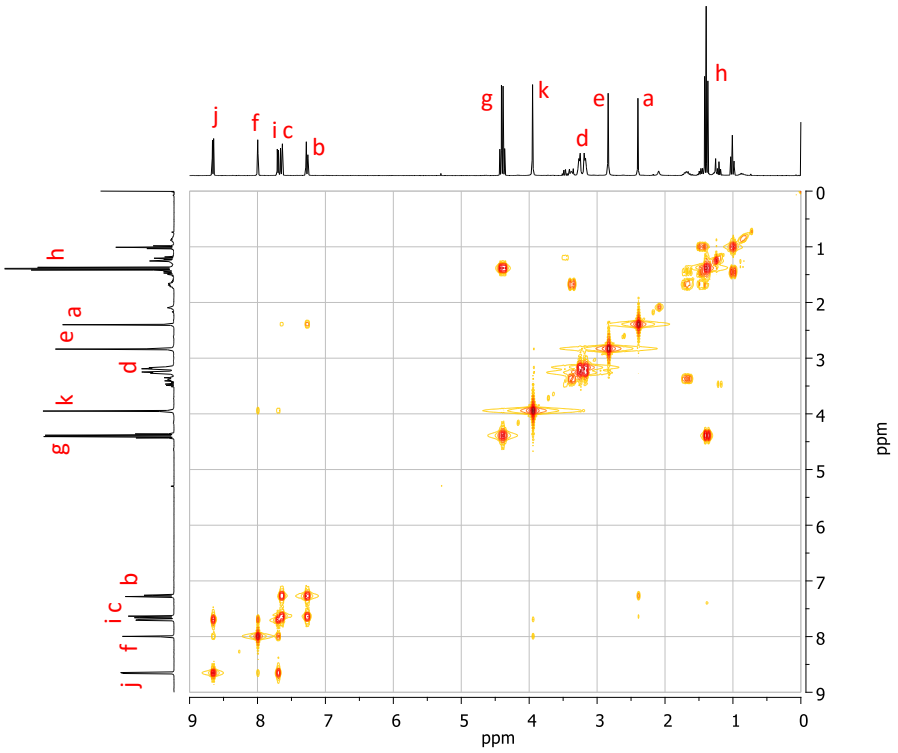

Figure SI. 1. ^{1}H-^{1}H COSY ($CDCl_3$, 400 MHz, 300 K) spectrum of $^{H,CO2Et}Py_2{}^{Ts}tacn$.

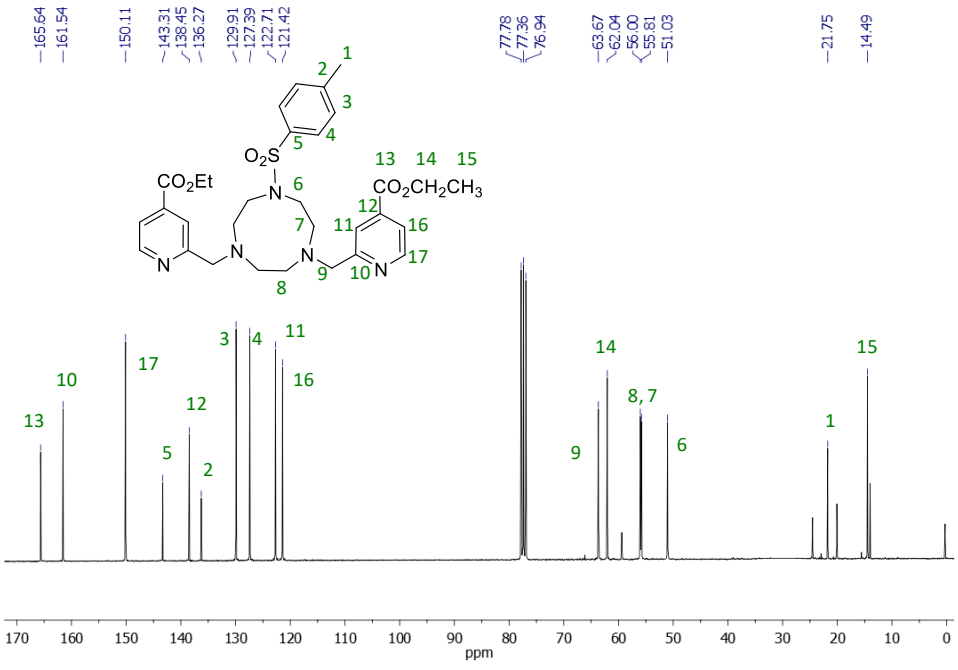

Figure SI. 2. $^{13}C\{^{1}H\}$-NMR ($CDCl_3$, 400 MHz, 300 K) spectrum of $^{Me,OMe}Py_2{}^{Ts}tacn$.

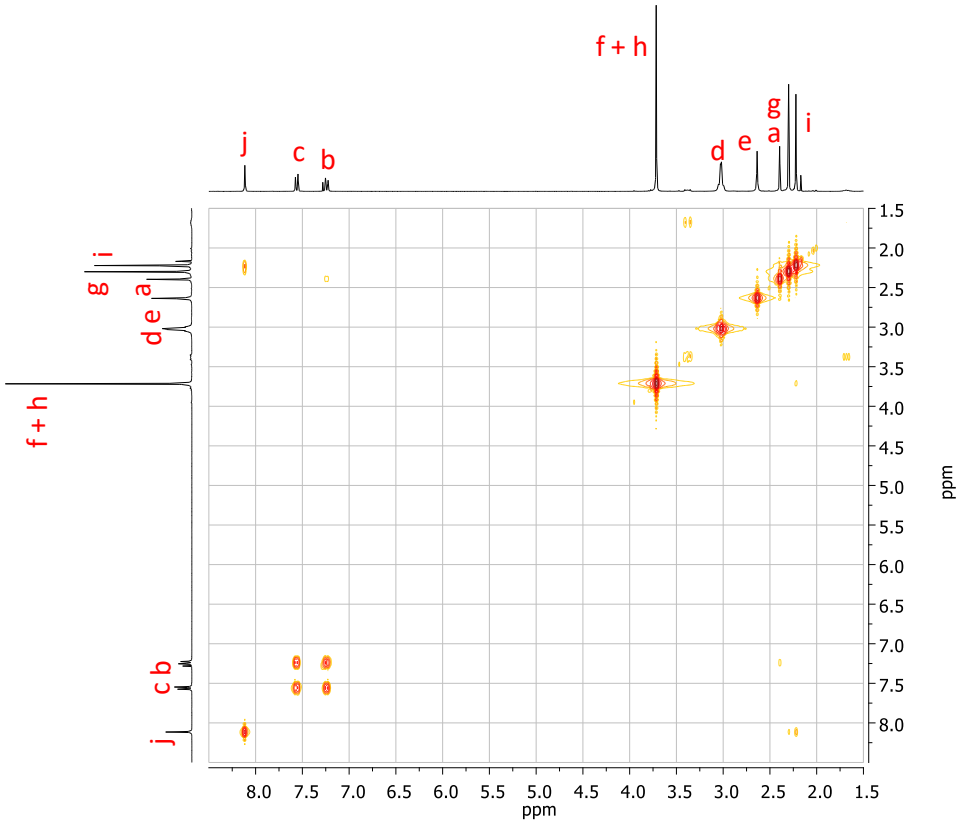

Figure SI. 3. ^{1}H-^{1}H COSY ($CDCl_3$, 400 MHz, 300 K) spectrum of $^{Me,OMe}Py_2{}^{Ts}$tacn.

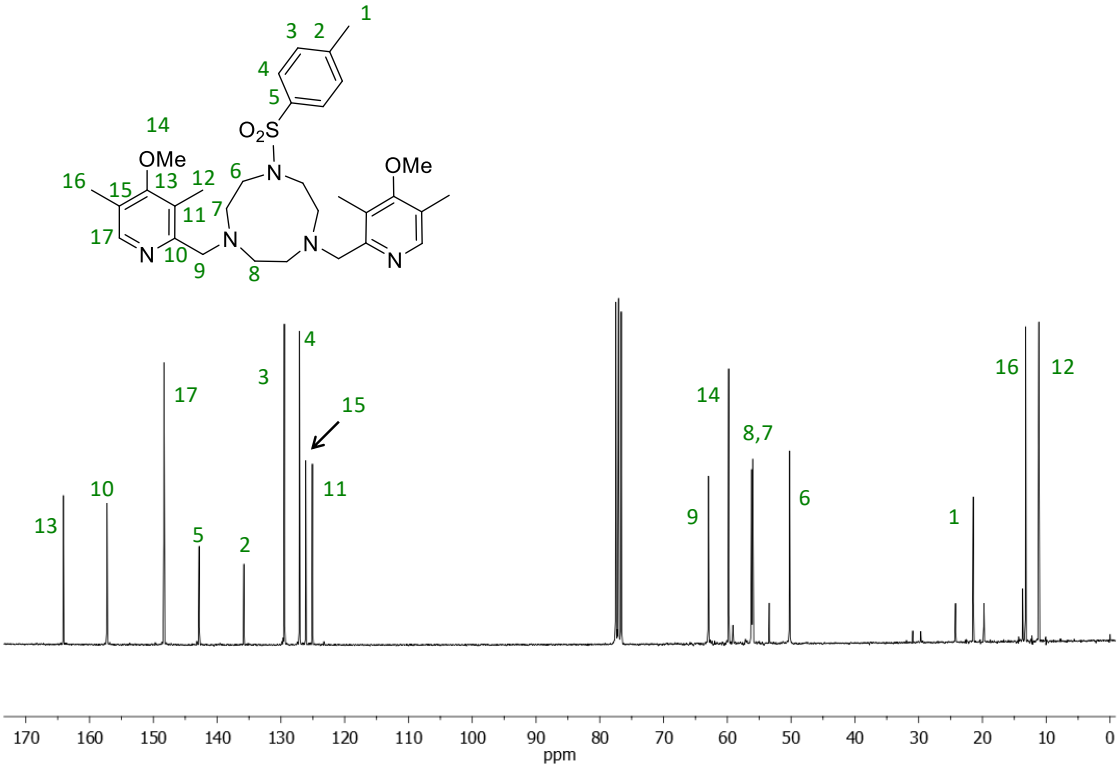

Figure SI. 4. ^{13}C{^{1}H} NMR ($CDCl_3$, 400 MHz, 300 K) spectrum of $^{Me,OMe}Py_2{}^{Ts}$tacn.

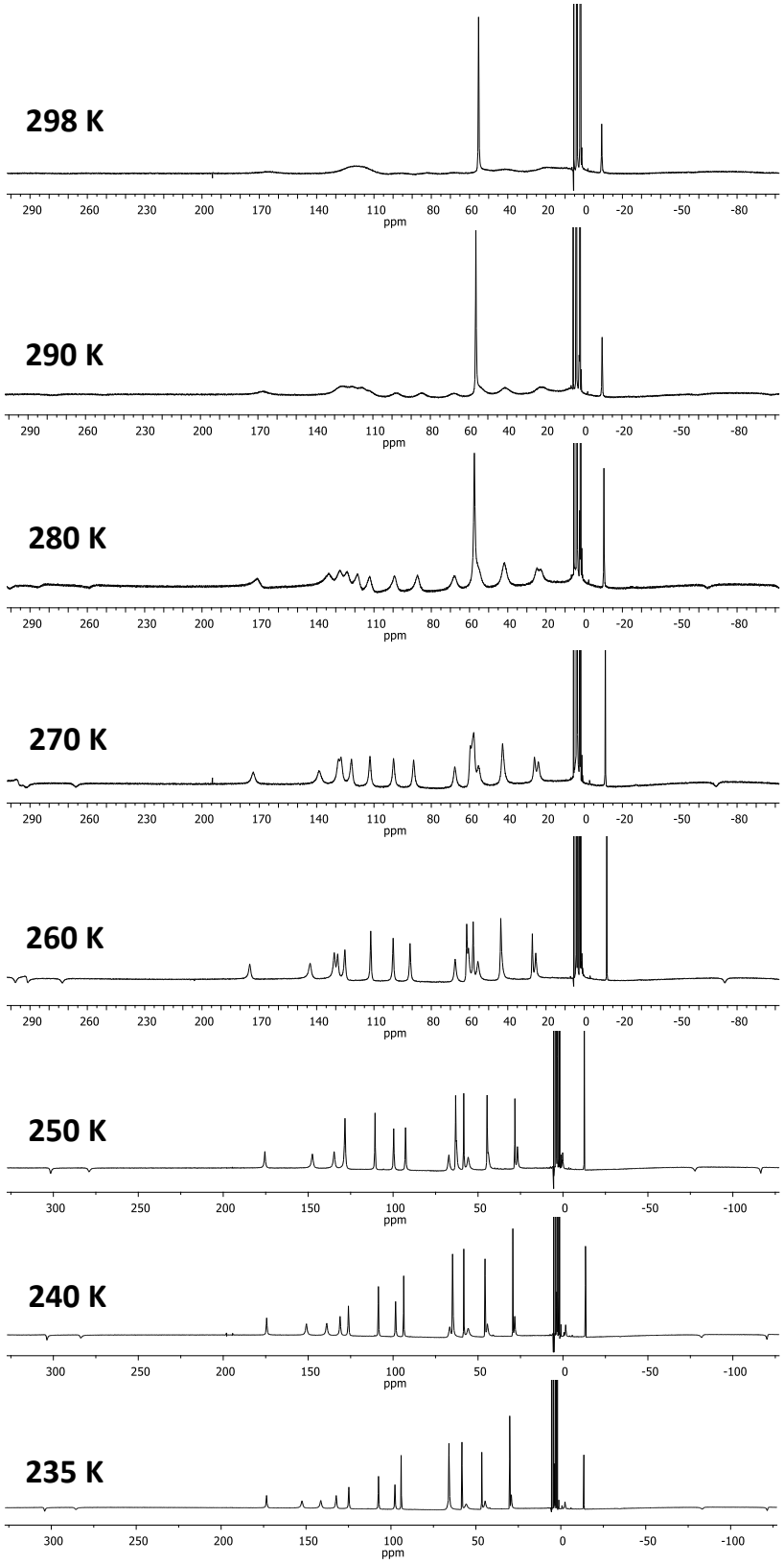

Figure SI. 5. ^{1}H-NMR spectra (500 MHz) of **1^{H}** in CD_3CN at different temperatures.

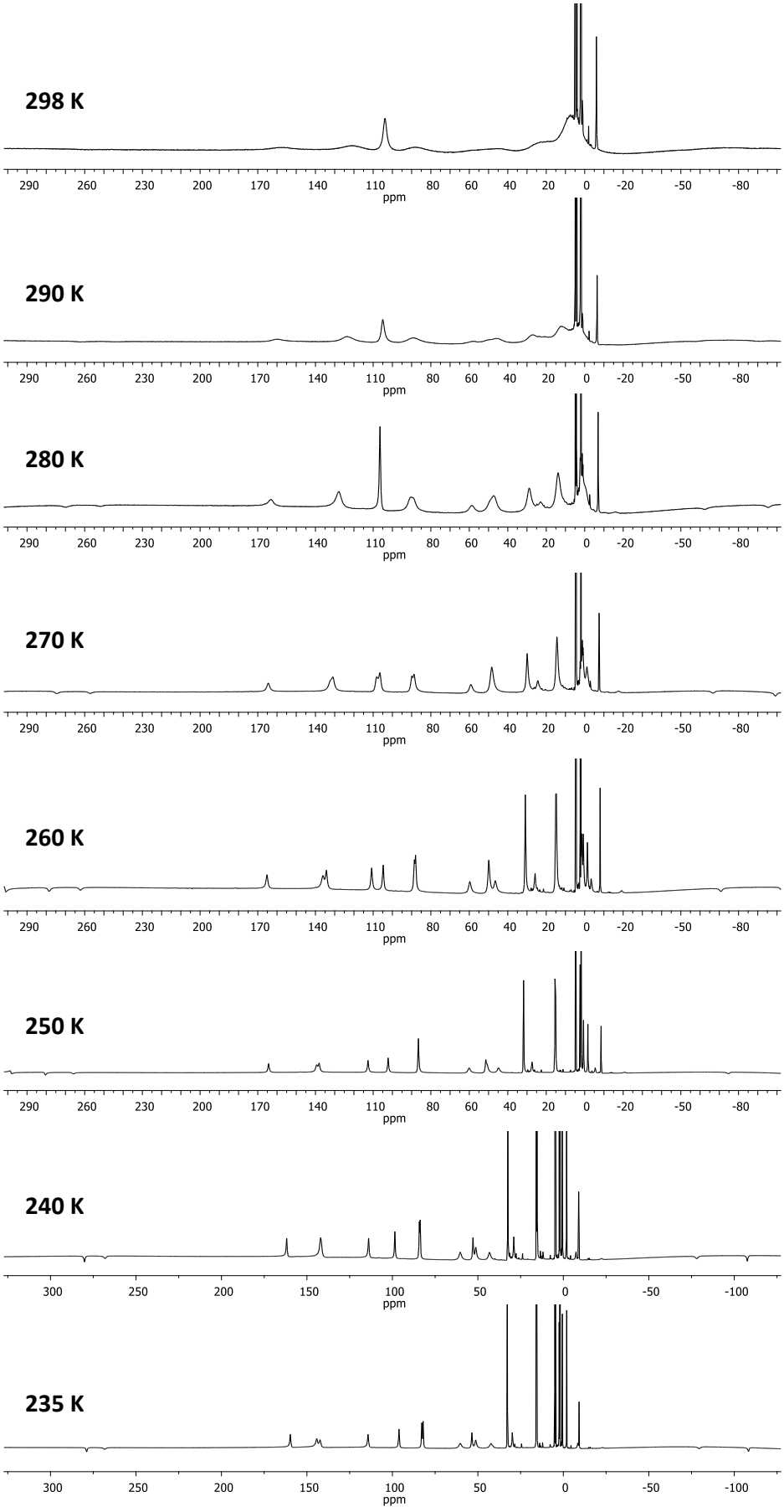

Figure SI. 6. ^{1}H-NMR spectra (500 MHz) of $\mathbf{1^{DMM}}$ in CD_3CN at different temperatures.

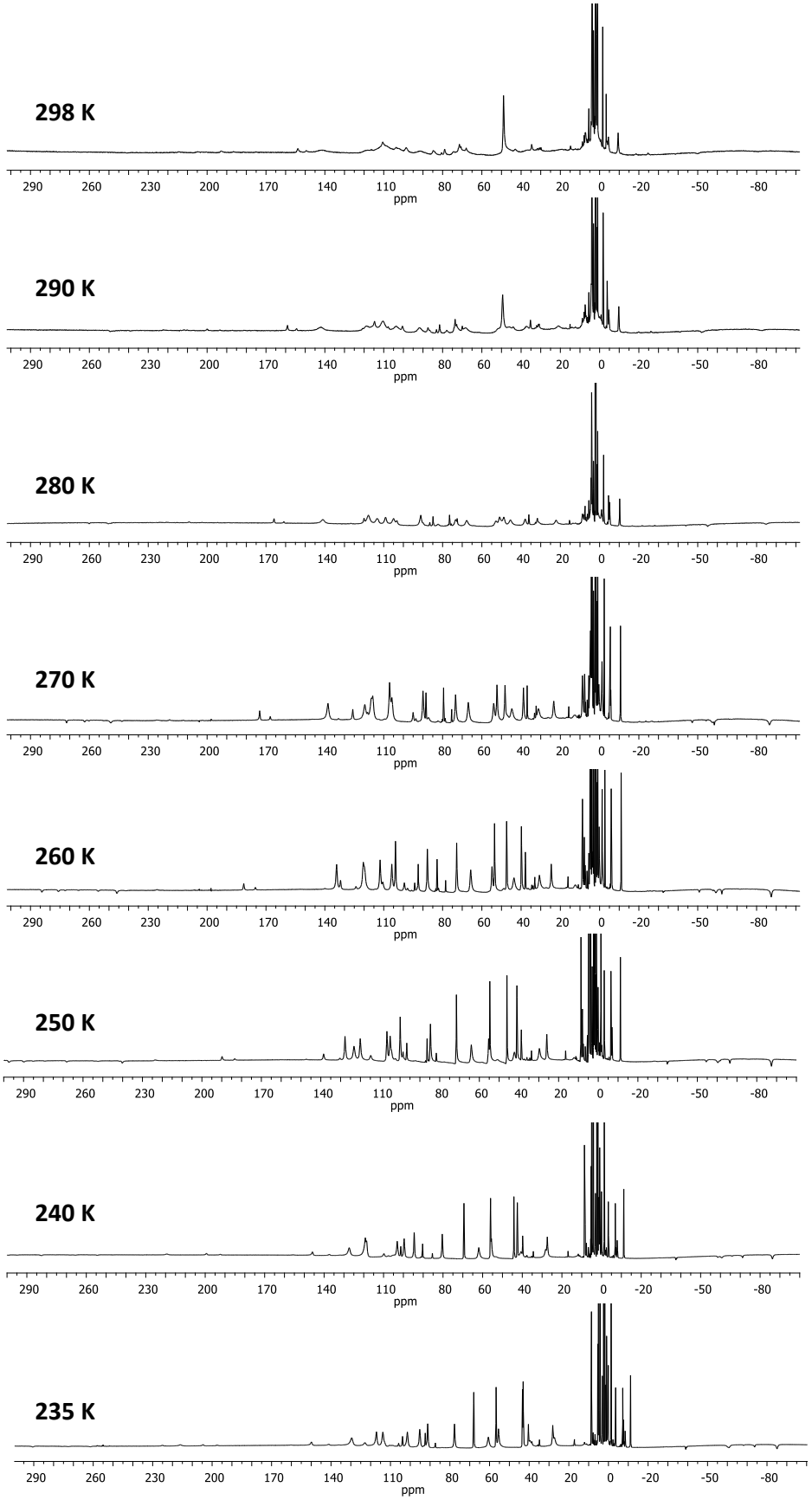

Figure SI. 7. ^{1}H-NMR spectra (500 MHz) of **1^{CO2Et}** in CD_3CN at different temperatures.

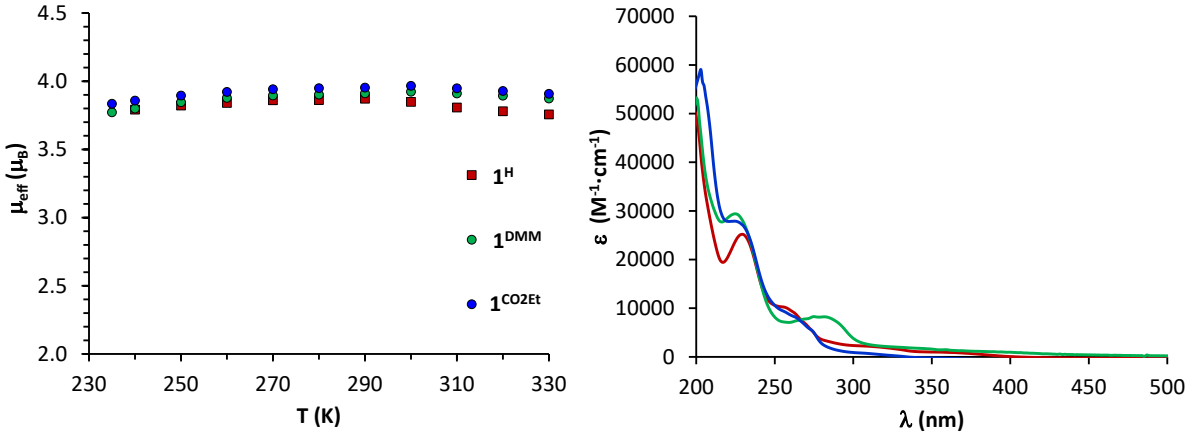

Figure SI. 8. Left: Representation of the effective magnetic moment of $\mathbf{1}^{CO2Et}$, $\mathbf{1}^{H}$ and $\mathbf{1}^{DMM}$ as a function of temperature. μ_{eff} values were obtained in CD_3CN using the Evans' method.[4] Right: UV/Vis absorption spectra of a 50 μM solution of $\mathbf{1}^{CO2Et}$ (blue), $\mathbf{1}^{H}$ (red) and $\mathbf{1}^{DMM}$ (green) in MeCN at 298 K.

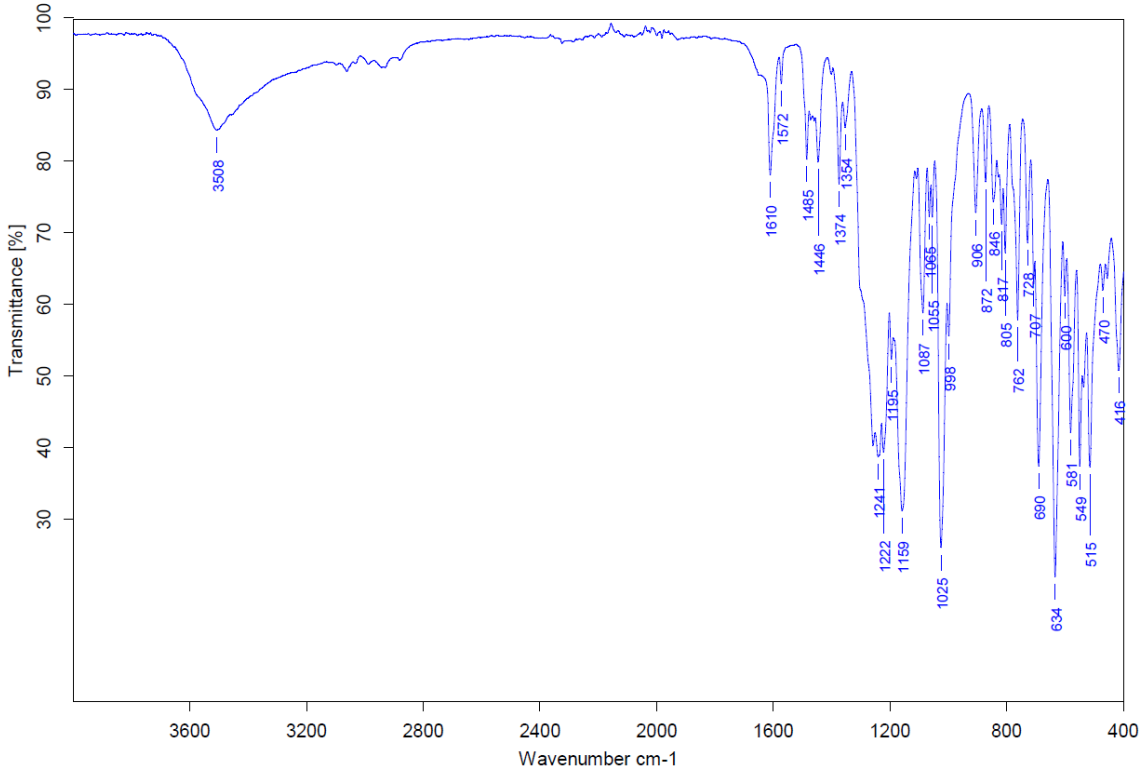

Figure SI. 9. FIT-IR spectrum of $\mathbf{1}^{H}$.

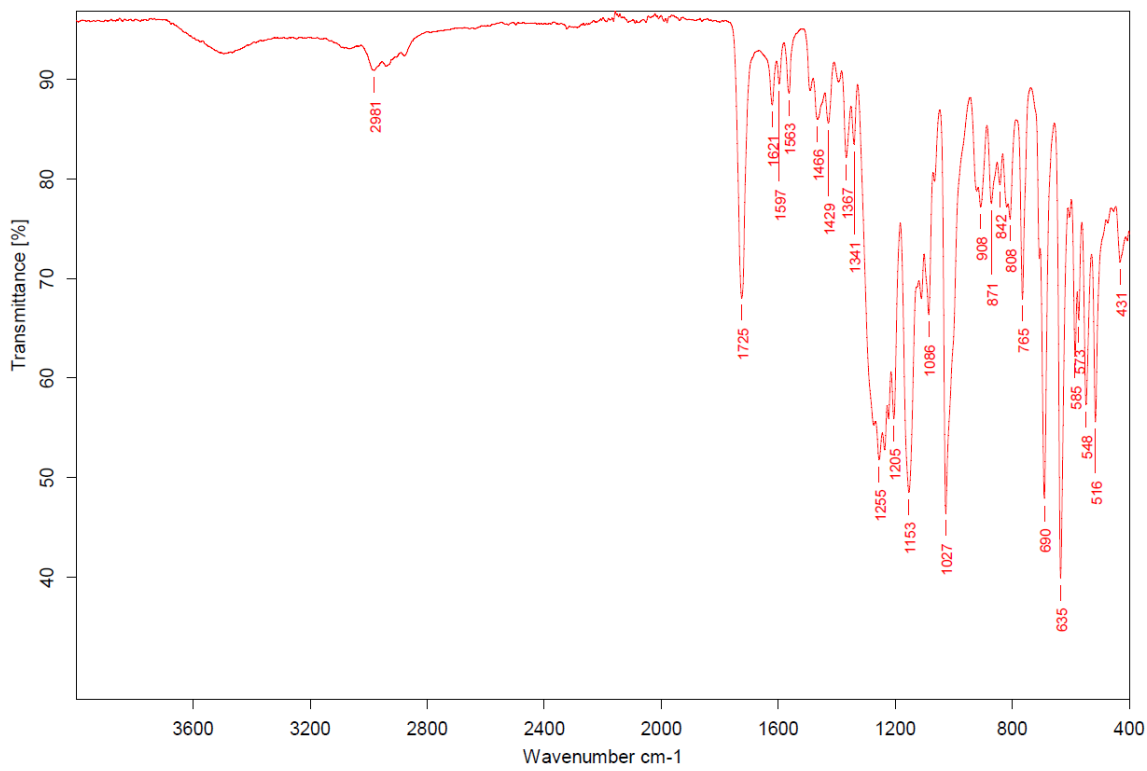

Figure SI. 10. FIT-IR spectrum of **1**^{CO2Et}.

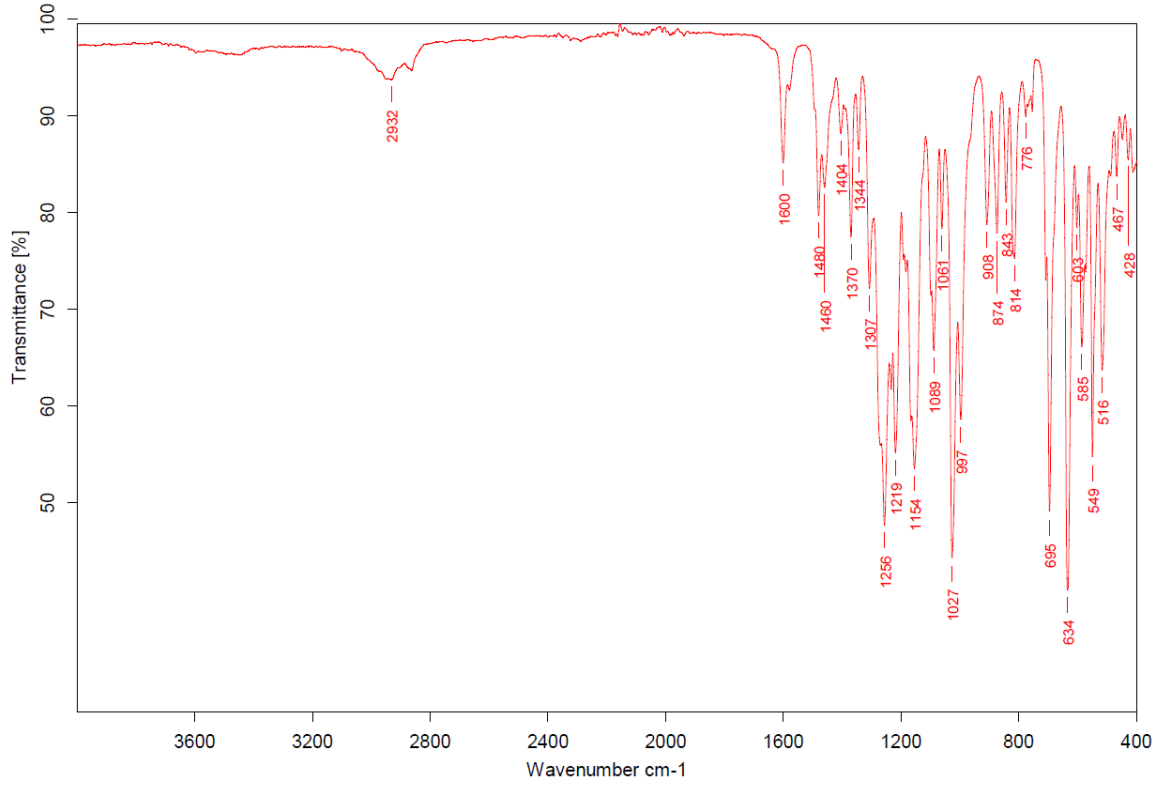

Figure SI. 11. FIT-IR spectrum of **1**^{DMM}.

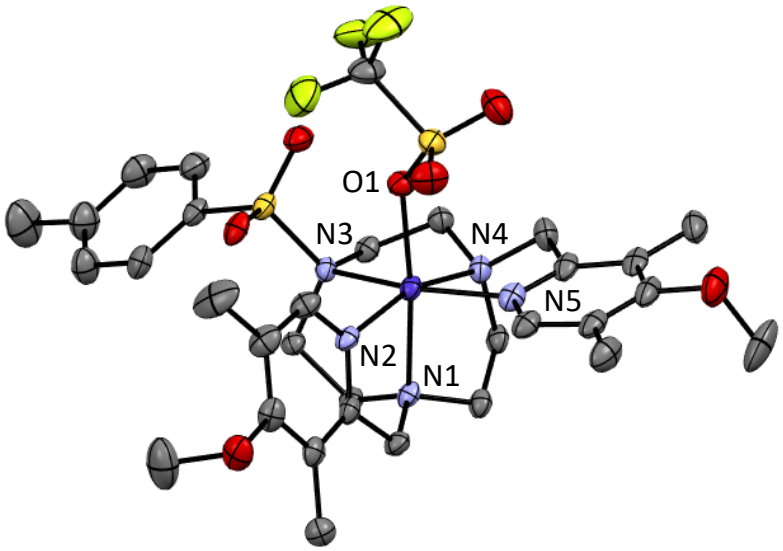

Figure SI. 12. Crystal structures of the cobalt complexes $\mathbf{1}^{DMM}$ (50 % probability). Solvent molecules and hydrogen atoms are omitted for clarity. Color code: cobalt (blue), nitrogen (light blue), oxygen (red), fluor (yellow), carbon (grey) and sulfur (orange).

Table SI. 1. Crystal Data for $\mathbf{1^{DMM}}$.

Compound	$\mathbf{1^{DMM}}$
Empirical formula	$C_{38.25}H_{47.50}CoF_{7.50}N_5O_{10}S_3$
Formula weight	1088.09
Temperature	100(2) K
Wavelength	0.71073 Å
Crystal system	Monoclinic
Space group	Cs/c
Unit cell dimensions	a = 42.0464(14) Å
	α = 90°
	b = 9.0171(3) Å
	β = 124.4553(11)°
	c = 29.4652(11) Å
	γ = 90°
Volume	9211.5(6) Å^3
Z	8
Density (calculated)	1.569 Mg/m^3
Adsorption coefficient	0.686 mm^{-1}
F(000)	4480
Crystal size	0.20 x 0.04 x 0.02 mm^3
Θ range for data collection	1.175 to 25.076°
Index ranges	-43 ≤ h ≤ 50
	-10 ≤ k ≤ 10
	-35 ≤ l ≤ 27
Reflections collected	49533
Independent reflections	8166
	[R(int) = 0.0592]
Completeness to Θ	99.9 % (Θ = 25.076°)
Absorption correction	Multi-scan
Max. and min. transmission	0.986 and 0.891
Refinement method	Full-matrix least-squares on F^2
Data / restraints / parameters	8166/348/755
Goodness-of-fit on F^2	1.069
Final R indices [I>2α(I)]	R1 = 0.0602
	wR2 = 0.1497
R indices (all data)	R1 = 0.0892
	wR2 = 0.1669
Largest diff. peak and hole	0.949 and -1.042 e·Å^{-3}

Table SI. 2. Selected Bond Lengths (Å) and Angles (°) for $\mathbf{1}^{DMM}$.

$\mathbf{1}^{DMM}$	
Co-N1	2.142(4)
Co-N2	2.071(4)
Co-N3	2.326(4)
Co-N4	2.113(4)
Co-N5	2.123(4)
Co-O1	2.058(3)
N1-Co-N2	79.69(14)
N1-Co-N3	81.85(13)
N1-Co-N4	82.96(14)
N1-Co-N5	96.46(14)
N1-Co-O1	173.16(13)
N2-Co-N3	99.57(13)
N2-Co-N4	162.40(14)
N2-Co-N5	99.50(15)
N2-Co-O1	99.70(13)
N3-Co-N4	80.78(13)
N3-Co-N5	160.21(14)
N3-Co-O1	91.57(12)
N4-Co-N5	79.45(14)
N4-Co-O1	97.88(14)
N5-Co-O1	90.36(14)

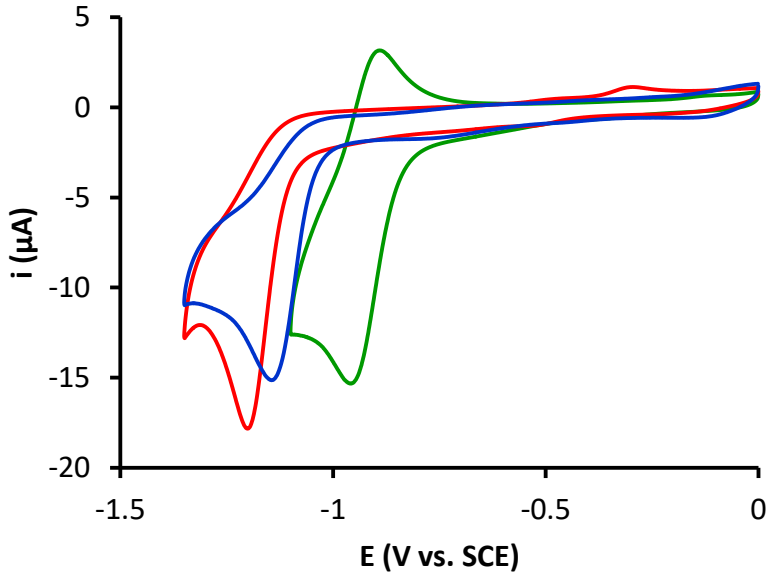

Figure SI. 13. CVs of $\mathbf{1}^{CO2Et}$ (green), $\mathbf{1}^{H}$ (blue) and $\mathbf{1}^{DMM}$ (orange) at 1 mM in MeCN with 0.1 M Bu_4NPF_6 as supporting electrolyte, using a glassy carbon working electrode and a SCE reference electrode. Scan rate of 100 mV s^{-1}.

6. Photocatalytic experiments

6.1. Photocatalytic water reduction to H_2.

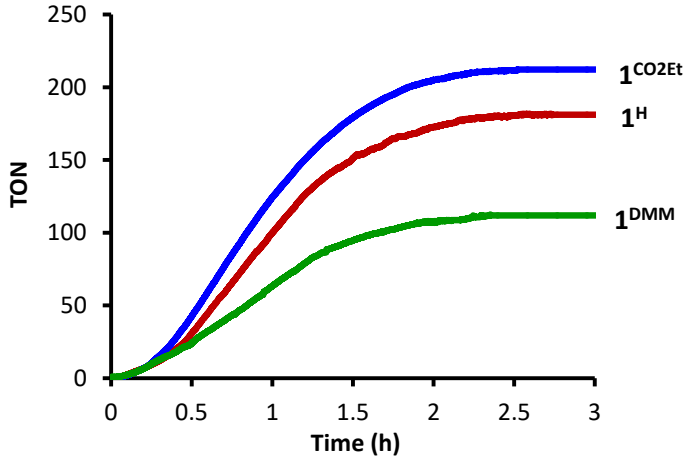

Figure SI. 14. On-line hydrogen evolved versus time with the cobalt complexes (50 μM), **PS$_{Ir}$** (250 μM) using CH_3CN:H_2O:Et_3N (2:8:0.2 mL) as solvent and irradiated (λ = 447 nm) at 25 ºC. **1^{CO2Et}** (blue), **1^{H}** (red), **1^{DMM}** (green). TON = $n(H_2)/n$(**Cat**).

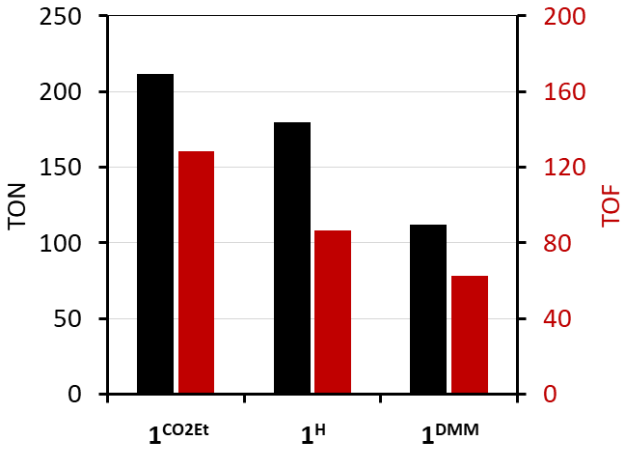

Figure SI. 15. H_2 evolution photocatalytic activity of the pentadentate cobalt complexes. Conditions: **1^{R}** (50 μM), **PS$_{Ir}$** (250 μM) using CH_3CN:H_2O:Et_3N (2:8:0.2 mL) as solvent and irradiated (λ = 447 nm) at 25 ºC under N_2.

6.2. Cobalt salts screening

Catalytic experiments with $[Co^{II}(OTf)_2(MeCN)_2]$, $Co^{II}SO_4$, $Co^{II}(OAc)_2$, $Co^{II}(acac)_2$, $Co^{II}Cl_2$ and $Co^{II}(NO_3)_2$ cobalt salts lead to negligible amounts of **3b** (< 4 % yield) and H_2 (< 3 % respect to the obtained in the presence of the ligand) (**Table SI. 3**). Likewise, ligand Py_2^{Ts}tacn alone was not found catalytically active. However, when an equimolar addition of Py_2^{Ts}tacn ligand cobalt metal salt was directly added to the reaction mixture just before irradiation, the formation of **3b** was observed with similar yields to the preformed $\mathbf{1^H}$ (53-66 % vs. 65 %) (Figure SI. 16), regardless the anion used. In addition, the combination of $[Co(OTf)_2(MeCN)_2]$ with two or higher stoichiometric amounts of Py_2^{Ts}tacn reduce the reaction yield. This fact can be rationalized by the saturation of the cobalt coordination sphere. All these results together provides evidences that the Py_2^{Ts}tacn cobalt complexes with free sites are the main responsible for the catalysis, and it cannot be attributed to free metal in solution. Arguably, the cobalt complex $\mathbf{1^H}$ is directly responsible for the ketone reduction.

Table SI. 3. Cobalt salts screened in presence and absence of Py_2^{Ts}tacn ligand and substrate **3a**.

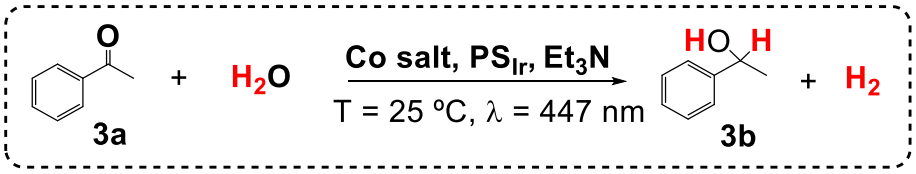

Cobalt salt precursor	[3a] (μmol)	Py_2^{Ts}tacn (n eq.)	H_2 (mL)	H_2 (μmol)	3b (μmol)	3b yield (%)	H_2 + 3b (μmol)
$Co^{II}SO_4$	165	-	<0.001	0.03	4.5	**3**	4.5
	165	1	1.5	59	95	**57**	155
	-	1	4.1	169	-	**-**	-
$Co^{II}(OAc)_2$	165	-	<0.001	0.02	4.2	**2**	4.2
	165	1	1.3	54	104	**62**	158
	-	1	3.5	142	-	**-**	-
$Co^{II}(acac)_2$	165	-	0	0	7.5	**5**	7.5
	165	1	1.5	59	98	**58**	157
	-	1	3.9	162	-	**-**	-
$Co^{II}Cl_2$	165	-	0.1	1.7	1.9	**1**	3.6
	165	1	1.4	57	92	**55**	150
	-	1	3.7	150	-	**-**	-
$Co^{II}(NO_3)_2$	165	-	0.03	1.1	5.5	**3**	6.6
	165	1	1.3	51	90	**53**	141
	-	1	3.4	140	-	**-**	-
$Co^{II}(OTf)_2$	165	-	0.01	0.2	6.7	**4**	7.2
	165	1	1.5	62	109	**66**	171
	165	2	1.0	42	94	**56**	136
	165	3	0.7	30	74	**44**	104
	165	4	0.5	22	59	**35**	81
	-	1	4.2	172	-	**-**	-

Reaction conditions: [**3a**] (0.168 mmol, 16.5 mM), $\mathbf{PS_{Ir}}$ (2.5 μmol, 1.5 mol%), Co^{II} salts (5 μmol, 3 mol%), MeCN:H_2O: Et_3N (2:8:0.2 mL), irradiating at λ = 447 nm for 5 h at 25 ºC under N_2.

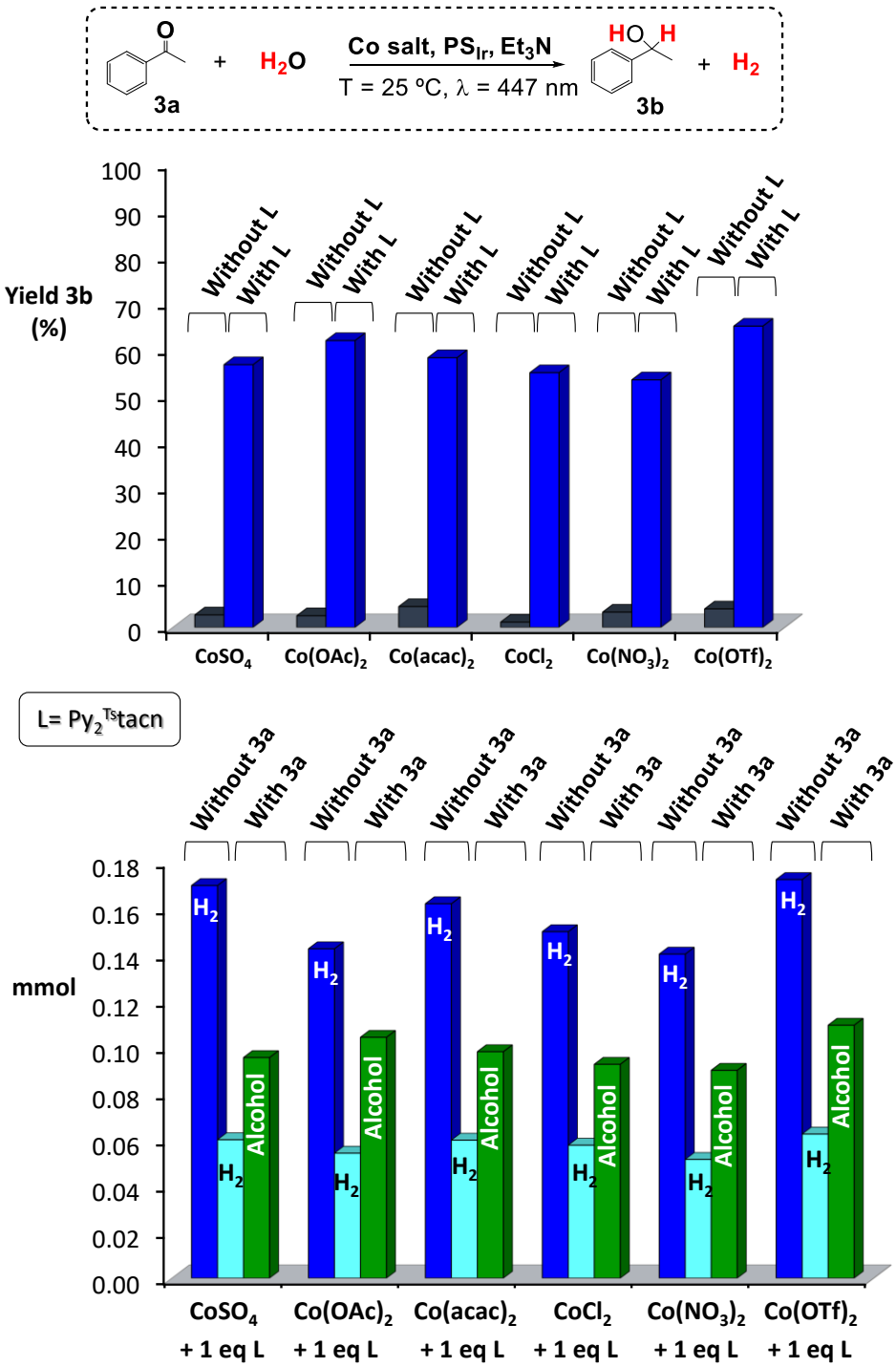

Figure SI. 16. *Top:* Effect of the presence of the ligand $Py_2^{Ts}tacn$. Photocatalytic acetophenone reduction to **3b** using different cobalt salts in the absence (dark blue columns) and in the presence of 1 eq. of ligand (L=$Py_2^{Ts}tacn$) (blue columns). The addition of ligand give rise to a substantial improvement of yield. *Bottom:* Mmol of H_2 and **3b** produced with different cobalt salts in the presence of $Py_2^{Ts}tacn$. *Dark blue*: mmol of H_2 produced in the absence of **3a**. *Light blue*: mmol of H_2 produced in the presence of **3a**. *Green:* mmol of **3a** produced. Reaction conditions: [**3a**] (0.168 mmol, 16.5 mM), $\mathbf{PS_{Ir}}$ (2.5 μmol, 1.5 mol%), **cobalt salt** (5 μmol, 3 mol%), MeCN:H_2O: Et_3N (2:8:0.2 mL), irradiating at λ = 447 nm for 5 h at 25 ºC under N_2. It should be noted that the total amount of mmol of products is similar in the presence and absence of substrate for each catalytic system.

6.3. Photocatalytic activities of 1^R and 2^R complexes

Catalyst	E ($Co^{II/I}$) vs SCE	Yield **3b** (%)
$\mathbf{1}^{CO2Et}$	-0.96	18
$\mathbf{1}^{H}$	-1.14	65
$\mathbf{1}^{DMM}$	-1.20	68
$\mathbf{2}^{CO2Et}$	-1.15	15
$\mathbf{2}^{Cl}$	-1.33	30
$\mathbf{2}^{H}$	-1.36	36
$\mathbf{2}^{DMM}$	-1.38	44
$\mathbf{2}^{NMe2}$	-1.44	48

Table SI. 4. Summary of the acetophenone (**3a**) reduction by $\mathbf{1}^R$ and $\mathbf{2}^R$ under the following conditions: $\mathbf{1}^R$ (5 μmol, 3 mol%), $\mathbf{PS}_{Ir}$ (2.5 μmol, 1.5 mol%), **3a** (16.5 mM) in a CH_3CN:H_2O:Et_3N (2:8:0.2 mL) solvent mixture and irradiated (λ = 447 nm) at 25 ºC under N_2 for 4 h.

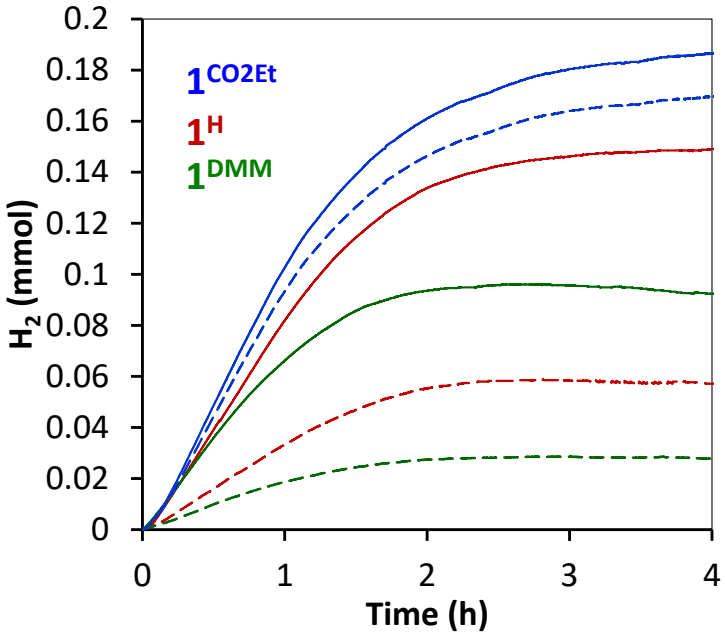

Figure SI. 17. Online monitoring of the photocatalytic H_2 production in the absence (solid line) and presence of **3a** (0.168 mmol, 16.5 mM) (dashed line) for $\mathbf{1}^{CO2Et}$ (blue), $\mathbf{1}^{H}$ (red) and $\mathbf{1}^{DMM}$ (green). Conditions: $\mathbf{1}^R$ (5 μmol, 3 mol%), $\mathbf{PS}_{Ir}$ (2.5 μmol, 1.5 mol%) in a CH_3CN:H_2O:Et_3N (2:8:0.2 mL) solvent mixture and irradiated (λ = 447 nm) at 25 ºC under N_2 for 4 h.

Table SI. 5. H_2 and **3b** formed in the absence and presence of **3a** (0.168 mmol, 16.5 mM) under the following conditions: $\mathbf{1^R}$ (5 μmol, 3 mol%), $\mathbf{PS_{Ir}}$ (2.5 μmol, 1.5 mol%) in a CH_3CN:H_2O:Et_3N (2:8:0.2 mL) solvent mixture and irradiated (λ = 447 nm) at 25 ºC under N_2 for 4 h

Cat	[3a] (mmol)	H_2 (mmol)	Initial Rate H_2 ($mmol \cdot h^{-1}$)	3b (mmol)	Initial Rate 3b ($mmol \cdot h^{-1}$)	Ratio ($H_2(3a)/H_2$	Selectivity ($3b/H_2$)
$\mathbf{1^{CO2Et}}$	0	0.193	0.091	-	-	**0.91**	0.2
	0.168	0.175	0.082	0.030	0.010		
$\mathbf{1^{H}}$	0	0.151	0.084	-	-	**0.39**	1.9
	0.168	0.059	0.032	0.109	0.066		
$\mathbf{1^{DMM}}$	0	0.096	0.071	-	-	**0.30**	3.9
	0.168	0.032	0.018	0.113	0.067		

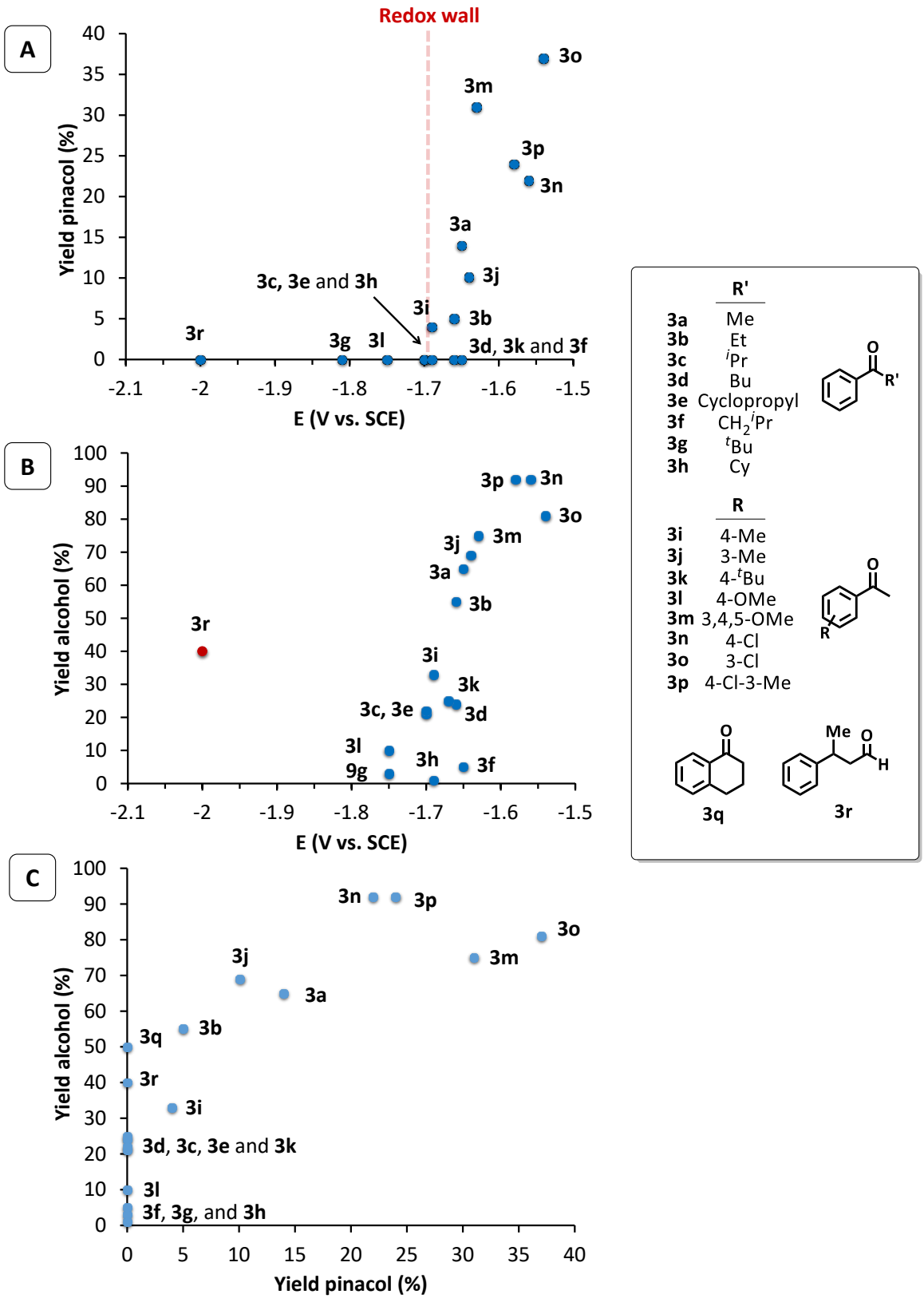

Figure SI. 18. Correlation between A) Yield pinacol-redox potential substrate. B) Yield alcohol-redox potential substrate. C) Yield alcohol-yield pinacol. The yields of alcohol are determined in the presence of $\mathbf{1}^{H}$ catalyst. The yield of pinacol are determined in the absence of $\mathbf{1}^{H}$.

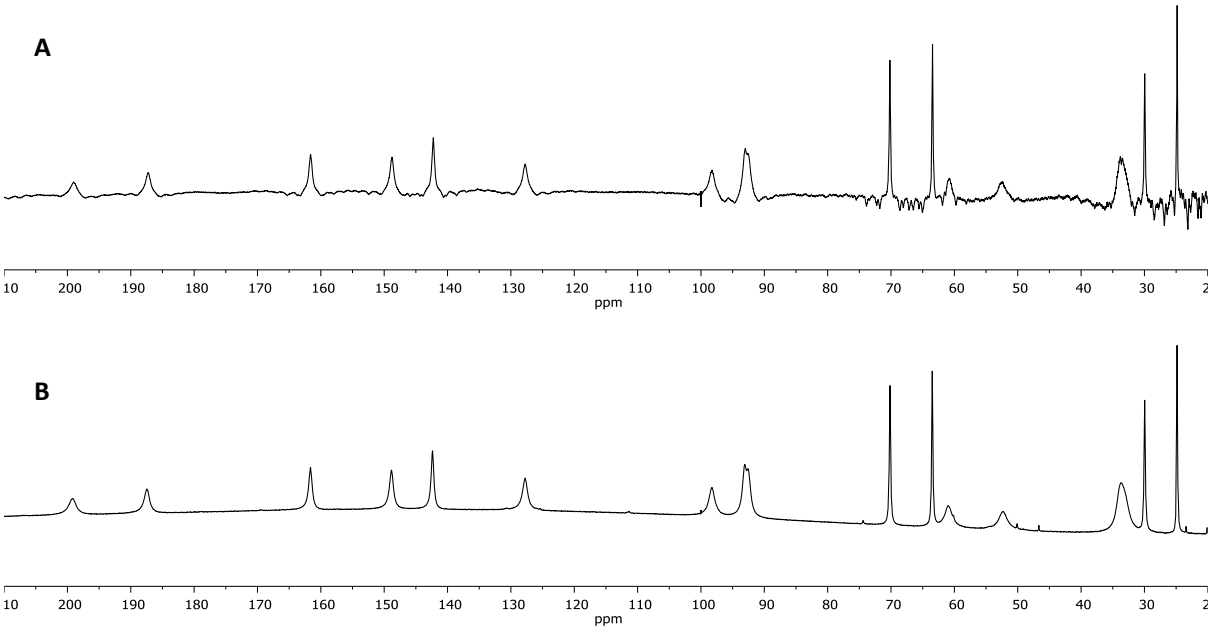

Figure SI. 19. ^{1}H-NMR spectra of **1^{H}** (25 mM) in CD_3CN:D_2O:Et_3N (2:8:0.2) before (A) and after (B) 12 h irradiation.

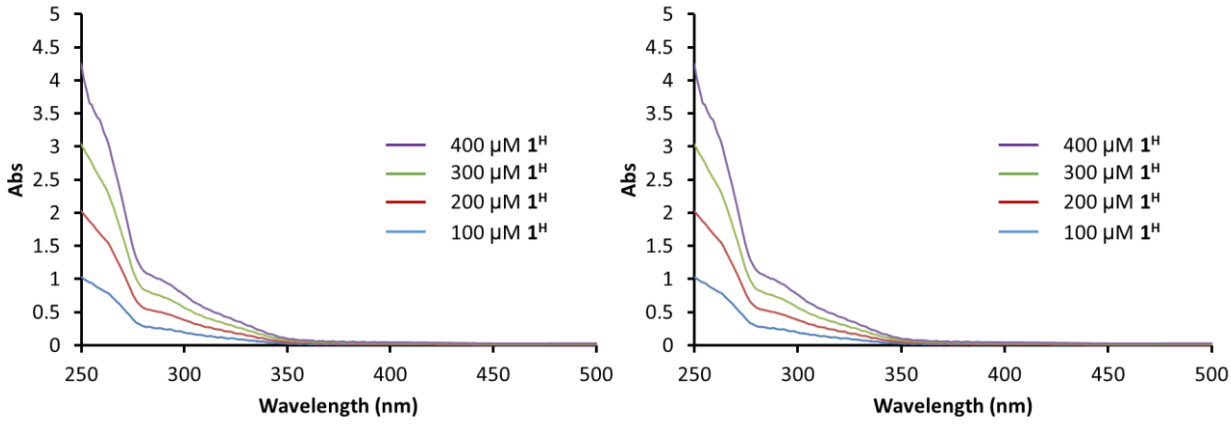

Figure SI. 20. UV/Vis spectra at different concentrations of **1^{H}** in the mixture CH_3CN:H_2O:Et_3N (2:8:0.2) before (*left*) and after 12 h irradiation (*right*).

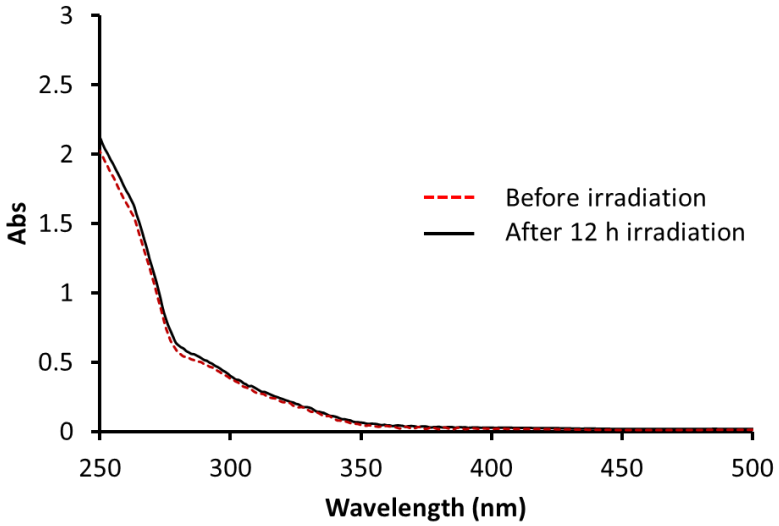

Figure SI. 21. UV/Vis spectra of $\mathbf{1^H}$ (200 μM) in the mixture CH_3CN:H_2O:Et_3N (2:8:0.2) before and after 12 h irradiation

References

(1) Cline, E. D.; Adamson, S. E.; Bernhard, S. *Inorg. Chem.* **2008**, *47*, 10378.
(2) Luo, S.-P.; Mejía, E.; Friedrich, A.; Pazidis, A.; Junge, H.; Surkus, A.-E.; Jackstell, R.; Denurra, S.; Gladiali, S.; Lochbrunner, S.; Beller, M. *Angew. Chem. Int. Ed.* **2013**, *52*, 419.
(3) Lloret-Fillol, J.; Codolà, Z.; Garcia-Bosch, I.; Gómez, L.; Pla, J. J.; Costas, M. *Nat. Chem.* **2011**, *3*, 807
(4) Evans, D. F. *J. Chem. Soc.* **1959**, 2003.